

Critical behavior of nonequilibrium models with infinitely many absorbing states

Iwan Jensen

Department of Mathematics, The University of Melbourne,
Parkville, Victoria 3052, Australia.
e-mail: iwan@maths.mu.oz.au

February 1, 2008

Abstract

I study the critical behavior of a two-dimensional dimer-trimer lattice model, introduced by Köhler and ben-Avraham [J. Phys. A **24**, L621 (1991)], for heterogeneous catalysis of the reaction $\frac{1}{2}A_2 + \frac{1}{3}B_3 \rightarrow AB$. The model possesses infinitely many absorbing states in which the lattice is saturated by adsorbed particles and reactions cease because only isolated vacancies are left. Results for various critical exponents show that the model exhibits the same critical behavior as directed percolation, contrary to earlier findings by Köhler and ben-Avraham. Together with several other studies, reviewed briefly in this article, this confirms that directed percolation is the generic universality class for models with infinitely many absorbing states.

PACS Numbers: 05.70.Ln, 05.50.+q, 64.90.+b

1 Introduction

The critical behavior of nonequilibrium lattice models with absorbing states has attracted a great deal of interest in recent years. It has been shown that most models exhibiting a continuous phase transition to a *unique* absorbing state belong to the same universality class. The best known examples are probably directed percolation (DP) [1], Reggeon field theory [2, 3], the contact process [4, 5], and Schlögl's first and second models [6]–[8]. Extensive studies of these and many other models [9]–[16] have revealed that the critical exponents are unaffected by a wide range of changes in the evolution rules. This provides firm support for the DP conjecture, first stated by Janssen [7] and Grassberger [8], that directed percolation is the generic critical behavior of models exhibiting a continuous transition into a unique absorbing state.

The study of models with more than one absorbing state is in an early stage, and there is still some controversy regarding the possible universality classes for such models. Models with *infinitely* many absorbing states arise naturally in the study of reactions catalysed by a surface as soon as the absorption mechanism for the various species requires more than one vacant site. Some studies of such models [17, 18, 19] in two dimensions indicated that they did not belong to the universality class of directed percolation. However, the exponent estimates varied significantly from model to model and could therefore not be consistent with just a single new universality class. While the exponent estimates quoted in some studies clearly ruled out DP critical behavior, those of other studies differed only marginally from the DP values. On the other hand, studies of several one-dimensional models [20, 21, 22] clearly placed these in the DP universality class, at least as far as the *static* critical behavior is concerned. In all of these models the number of absorbing configurations grows exponentially with system size, though the absorbing configurations are characterized by the vanishing of a unique quantity, e.g., the number of particle pairs [20] or in other cases [17, 18] the number of nearest neighbor vacancy pairs. Although there still is some evidence suggesting that models with infinitely many absorbing states may exhibit non-DP critical behavior, generally it seems that such models belong to the DP universality class. In this article I present results from a study of the dimer-trimer model, introduced by Köhler and ben-Avraham [17], which shows that this model, despite earlier evidence to the contrary, also belongs to the DP universality class. This result lends further support to the extensions of the DP conjecture to models with multiple components [24] and/or infinitely many absorbing states [20, 21], at least in cases where the absorbing states are characterized by the vanishing of a unique quantity.

The remainder of this article is organised as follows. In Section 2 I will briefly present the various models and review the results of previous studies. I will present the results from my study of the dimer-trimer in Section 3 and summarise and discuss the evidence regarding universality in Section 4.

2 Models with infinitely many absorbing states.

The dimer-trimer lattice model for heterogeneous catalysis for the reaction $\frac{1}{2}\text{A}_2 + \frac{1}{3}\text{B}_3 \rightarrow \text{AB}$ was introduced by Köhler and ben-Avraham [17]. Adsorption of dimers (trimers) is attempted with probability p ($1-p$) and succeeds if the molecule hits a pair (triplet) of nearest neighbor empty sites. Immediately upon adsorption the dimer (trimer) dissociates and each site of the pair (triplet) becomes occupied by one A (B) particle. If A and B particles happen to become nearest neighbors they react and the AB product desorbs at once, leaving behind two empty sites. Configurations with only isolated empty sites and adsorbed particles are absorbing; the number of such configurations grows exponentially with lattice size. Simulations [17] revealed that when $p < p_1$ the system enters a trimer-saturated state with only adsorbed B particles and isolated empty sites. Likewise a dimer-saturated state is reached for $p > p_2$, and only for intermediate values does the system possess an active steady state in which the production of AB goes on indefinitely. The transition at $p_1 = 0.3403(2)$ is continuous whereas the transition at $p_2 = 0.4610(8)$ is discontinuous. Critical exponents β_A and β_B describing, respectively, the behavior of the density of A and B particles near p_1 may be defined as: $\rho_A \propto |p - p_1|^{\beta_A}$ and $\rho_B^{sat} - \rho_B \propto |p - p_1|^{\beta_B}$, where ρ_B^{sat} is the saturation concentration of B at p_1 . Steady state computer simulations [17] yielded $\beta_A = 0.80(6)$ and $\beta_B = 0.63(5)$. For directed percolation in (2+1)-dimensions $\beta = 0.592(10)$ (this estimate is obtained using the scaling relation $\beta = \delta\nu_{\parallel}$ [5] with $\delta = 0.460(6)$ and $\nu_{\parallel} = 1.286(5)$ [25]). While the estimate for β_A is well above the DP value the estimate for β_B is marginally consistent with it. The dimer-trimer model was also studied using time-dependent simulations. The general idea of time-dependent simulations is to start from a configuration which is very close to the absorbing state, and then follow the “average” time evolution of this configuration by simulating a large ensemble of independent realisations [5]. Out of the many possible (near-absorbing) initial states, Köhler and ben-Avraham used absorbing states *generated by the critical system*, and then placed a triplet of vacancies at the center (see the next section for more details). As usual in this type of simulation they measured the survival probability $P(t)$, the average number of empty sites $\bar{n}(t)$, and the average mean square distance of spreading $\bar{R}^2(t)$ from the origin. These quantities are expected to exhibit power-law behavior at p_1 characterized by exponents $-\delta$, η and z , respectively. The estimates for the dimer-trimer model [17], $\delta = 0.40(1)$, $\eta = 0.28(1)$, and $z = 1.19(1)$, clearly differ from the DP values [25], $\delta = 0.460(6)$, $\eta = 0.214(8)$ and $z = 1.134(4)$. These results led to the conclusion that the dimer-trimer model belongs to a new universality class. As already mentioned the results of my study of this model (reported in Section 3) do *not* support this conclusion but shows that the dimer-trimer model belongs to the DP universality class.

The dimer-dimer (DD) model [18] is based on the oxidation of hydrogen on a metal surface. O_2 adsorption is attempted with probability p , and H_2 adsorption with probability $1-p$. Both O_2 and H_2 require a nearest neighbor pair of vacancies; both dissociate

upon adsorption. Whenever H and O are nearest neighbors they react to form OH, which resides at a single site. Similarly, OH reacts with neighboring H, forming H₂O which desorbs immediately. In addition adsorbed H atoms are allowed to diffuse on the surface. The DD model has been studied in several versions including further processes such as, recombination and desorption of H₂, desorption of OH, and reactions between neighboring OH molecules (leading to the formation and desorption of H₂O leaving behind one adsorbed O atom). Depending on which processes are included the DD model exhibits one or two continuous phase transitions. For $p < p_1$, the steady state is absorbing and comprised of a mixture of O, OH and isolated vacancies. In certain versions of the model the lattice becomes saturated with H for $p > p_2$ – a unique absorbing state. For $p_1 < p < p_2$ there is an active steady state with ongoing production of H₂O. Monte Carlo simulations [18] generally yielded estimates for $\beta_X \simeq 1/2$ with an uncertainty of approximately 5-10%, where β_X describe the power-law decay of various densities at p_1 . However, in certain cases it was found [18] that $\beta_X \simeq 2/3$ or 1. Most of the results are not consistent with directed percolation and could indicate that the DD model belongs to a new universality class. However, one would expect the exponents, corresponding to different densities, to be equal. The difference in some of the reported values thus suggests substantial statistical uncertainties.

Jensen and Dickman studied two simpler models, the pair contact process (PCP) and the dimer reaction (DR) model, presenting infinitely many absorbing states in the simpler context of single-component, one-dimensional models [20, 21]. In the PCP, nearest neighbor pairs of particles annihilate mutually (with probability p) or else (with probability $1 - p$) create a new particle at an empty nearest neighbor. Any configuration without pairs is absorbing; there are evidently many such states ($> 2^{N/2}$ on a 1-d lattice of N sites). Steady state simulations, including a thorough finite-size scaling analysis, yielded exponent estimates consistent with DP critical behavior. In the one-dimensional DR, particles are not allowed to occupy neighboring sites. If sites i , $i - 1$ and $i + 1$ are vacant adsorption may take place at site i . Suppose a particle has just arrived at site i . If sites $i - 3$, $i - 2$, $i + 2$, and $i + 3$ are all vacant, the particle remains. If any of the four sites are occupied, the new particle reacts with one other particle with probability $1 - p$, and remains with probability p . The second neighbors have priority in the reaction. Any configuration without triplets of empty sites is absorbing. Again steady state simulations (including finite-size scaling) revealed critical behavior in the DP universality class.

Another single-component model which exhibits a continuous phase transition from an active steady state to one of a multitude of absorbing configurations is the *threshold transfer process* (TTP) [22]. In the TTP sites may be vacant, or singly or doubly occupied, which can be described by an occupation variable $\sigma_i = 0, 1$ or 2 . If $\sigma_i = 0$, then $\sigma_i \rightarrow 1$ with probability p ; if $\sigma_i = 1$, then $\sigma_i \rightarrow 0$ with probability $1 - p$. In the absence of doubly-occupied sites, the dynamics trivially leads to a steady state in which a fraction p of the sites have $\sigma_i = 1$. When $\sigma_i = 2$ particles may move to neighboring sites. If $\sigma_{i-1} < 2$, one particle moves to that site; likewise, a particle

moves from i to $i + 1$ if $\sigma_{i+1} < 2$. σ_i is diminished accordingly in this deterministic, particle-conserving transfer. Configurations devoid of doubly-occupied sites form an absorbing subspace with trivial dynamics and can be avoided only if p is sufficiently large. Simulations [22] revealed that the steady state critical behavior placed the TTP in the DP universality class.

Recently, Yaldrum *et al.*, studied the critical behavior of a model for the $\text{CO} + \text{NO} \rightarrow \text{CO}_2 + \frac{1}{2}\text{N}_2$ catalytic surface reaction. With probability p a CO molecule is adsorbed on an empty site and with probability $1 - p$ NO adsorption is attempted. NO dissociates upon adsorption and therefore requires a nearest neighbor pair of empty sites. After each adsorption the nearest neighbors are checked (in random order) and $\text{CO} + \text{O}$ reacts to form CO_2 which leaves the surface at once, likewise $\text{N} + \text{N}$ forms N_2 which desorbs immediately. Computer simulations by Yaldrum *et al.* [19] showed that when $p < p_1$ the system enters an absorbing state in which the lattice is covered by a mixture of O and N. Again, the number of absorbing configurations grows exponentially with system size. At p_1 the model exhibits a *continuous* phase transition into an active state in which the catalytic process can proceed indefinitely. Finally when p exceeds a second critical value p_2 the model exhibits a *discontinuous* phase transition into a CO and N covered state. Near the critical point p_1 one expects the concentrations ρ_X of various lattice sites X ($X = \text{O}, \text{N}, \text{CO}$, or an empty site) to follow simple power laws, $\rho_X - \rho_X^{\text{sat}} \propto (p - p_1)^{\beta_X}$, where ρ_X^{sat} is the saturation concentration. Yaldrum *et al.* [19] found that $\beta_X = 0.20 - 0.22$, which is much smaller than the DP value. This could indicate that the CO-NO model belongs to a new universality class. However a more thorough study [23] yielded exponent estimates consistent with DP critical behavior.

3 Results for the dimer-trimer model.

In this section I report the results of extensive time-dependent and steady state simulations of the dimer-trimer model including a thorough finite-size scaling analysis. The model was studied on a triangular lattice with each site either empty or occupied by a single A or B particle. In the actual simulations dimer (trimer) adsorption is attempted with probability p ($1 - p$). Close to the critical value p_1 the lattice soon becomes covered with B-particles. Since all processes depend on the presence of nearest neighbor pairs or triplets of empty sites an efficient algorithm uses a list of non-isolated empty sites or 'active' sites. By choosing the first site (randomly) from the list of active sites the time spent on failed adsorption attempts is greatly reduced. Dimer adsorption proceeds via choosing (at random) a nearest neighbor of the active site and placing A-particles on these sites if the second site is empty. For trimer adsorption two nearest neighbors of the active site are chosen such that the sites constitute the vertices of an equilateral triangle and adsorption takes place if all sites are empty. After each attempted adsorption the time variable is incremented by $1/N_a$, where N_a is the number

of active sites prior to the attempt. Each time step thus equals (on the average) one attempted update per lattice site. After each successful adsorption the neighbors of newly adsorbed particles are checked to see if A-B pairs were formed and such pairs are removed. If an A or B particle is part of more than one pair a random choice is made between the different A-B pairs.

3.1 Time-dependent behavior.

Time-dependent simulations [5] is generally the most efficient way of obtaining a precise estimate for the location of the critical point in models with absorbing states. The general idea is to study the average evolution of a system which initially is very close to an absorbing state. For models with a *unique* absorbing state this is a very simple procedure yielding accurate estimates for both the critical point and various critical exponents describing the critical power-law behavior of quantities such as the survival probability or the average number of active sites. For models with multiple absorbing state the situation is more intricate. A recent study [21] showed that the critical exponents depend upon the choice of initial configuration. However, two important facts emerged from this study, first of all the value of the *critical point* was always predicted correctly, and secondly by using an initial configuration generated by running the system at the critical point starting from an empty lattice the predictions for the dynamical critical exponents coincide with those expected from the static critical behavior. A recent more thorough study by Mendes *et al.* [22] confirmed this picture and led to a generalized scaling ansatz for models with multiple absorbing states. In this study I generate the initial configuration by simulating the dimer-trimer model on a 128×128 lattice (with periodic boundary conditions) at the value of p under investigation until it enters an absorbing state. An off-set (x, y) is then chosen randomly on this lattice. Hereafter the configuration is mapped cyclically onto a larger (512×512) lattice such that the state of site (i, j) on the large lattice is the same as that of site $(i + x \bmod 128, j + y \bmod 128)$ on the small lattice. Hereafter a triplet of nearest neighbor empty sites is placed at the origin. The size of the large lattice ensures that the cluster of empty sites grown from the seed at the origin never reaches the boundaries of the lattice. We thus start in a configuration close to an absorbing state (just three sites are open) and it should be close to a typical absorbing state of the infinite system. For each value of p I simulated 50 independent configurations and for each such configuration I simulated 5000 independent samples for a total of 250,000 samples. Each run had a maximal duration of 2000 time steps, but most samples entered an absorbing state before this limit was reached. I measured the survival probability $P(t)$ (the probability that the system has not entered an absorbing state at time t), the average number of active sites $\bar{n}(t)$, and the average mean square distance of spreading $\bar{R}^2(t)$ from the center of the lattice. Notice that $\bar{n}(t)$ is averaged over all runs whereas $\bar{R}^2(t)$ is averaged only over the surviving runs. In accordance with the scaling ansatz for models with a unique absorbing state [5, 25] one expects that these

quantities have the following scaling form,

$$P(t) \propto t^{-\delta} \Phi(\Delta t^{1/\nu_{\parallel}}), \quad (1)$$

$$\bar{n}(t) \propto t^{\eta} \Psi(\Delta t^{1/\nu_{\parallel}}), \quad (2)$$

$$\bar{R}^2(t) \propto t^z \Theta(\Delta t^{1/\nu_{\parallel}}), \quad (3)$$

where $\Delta = |p - p_1|$ is the distance from the critical point, and ν_{\parallel} is the correlation length exponent in the time direction. If Φ , Ψ , and Θ are non-singular at the origin then asymptotically ($t \rightarrow \infty$) $P(t)$, $\bar{n}(t)$, and $\bar{R}^2(t)$ behave as power-laws at p_1 with critical exponents $-\delta$, η , and z , respectively. Generally there are corrections to the pure power law behavior so that, e.g., $P(t)$ is more accurately given by [25]

$$P(t) \propto t^{-\delta}(1 + at^{-1} + bt^{-\delta'} + \dots) \quad (4)$$

and similarly for $\bar{n}(t)$ and $\bar{R}^2(t)$. More precise estimates for the critical exponents can be obtained if one looks at local slopes

$$-\delta(t) = \frac{\log[P(t)/P(t/m)]}{\log(m)}, \quad (5)$$

and similarly for $\eta(t)$ and $z(t)$. In a plot of the local slopes vs $1/t$ the critical exponents are given by the intercept of the curve for p_1 with the y -axis. The off-critical curves often have very notable curvature, i.e., one will see the curves for $p < p_1$ veering downward while the curves for $p > p_1$ veer upward. This enables one to obtain accurate estimates for p_1 and the critical exponents. In Fig. 1 I have plotted the local slopes for various values of p . From the plot of $\eta(t)$ it is clear that the two lower curves, corresponding to $p = 0.3418$, and 0.3420 , veer downward showing that $p_1 > 0.3420$. Likewise the upper curve, $p = 0.3424$, has a pronounced upward curvature. I therefore conclude that $p_1 = 0.3422(2)$. This estimate differs quite a bit from that of Köhler and ben-Avraham ($p_1 = 0.3403(3)$), which is probably due to slightly different algorithms. From the intercept of the critical curves with the y -axis I estimate $\delta = 0.46(1)$, $\eta = 0.225(5)$ and $z = 1.13(1)$. These values agree very well with those obtained from computer simulations of directed percolation in (2+1)-dimensions [25], $\delta = 0.460(6)$, $\eta = 0.214(8)$ and $z = 1.134(4)$.

From these results it seems reasonable to conclude that the dimer-trimer model belongs to the DP universality class. However, due to the somewhat arbitrary choice of the initial configuration employed in the time-dependent simulations it would be nice to

validate this conclusion through other means. To this end I have also performed extensive steady state simulations using a finite-size scaling analysis.

3.2 Finite-size scaling behavior.

Finite-size scaling, though originally developed for equilibrium systems, is also applicable to nonequilibrium second-order phase transitions as demonstrated by Aukrust *et al.* [11]. As in equilibrium second-order phase transitions one assumes that the (infinite-size) system features a length scale which diverges at criticality as, $\xi(p) \propto \Delta^{-\nu_\perp}$, where ν_\perp is the correlation length exponent in the space direction. The basic finite-size scaling ansatz is that the various quantities depend on system-size only through the scaled length L/ξ , or equivalently through the variable $\Delta L^{1/\nu_\perp}$, where L is the linear extension of the system. Near the critical point p_1 one would expect the steady state concentrations ρ_X of various lattice sites X , $X = A, B$, active sites or empty sites (note that empty sites include only the isolated vacancies), to follow simple power laws,

$$|\rho_X^{sat} - \rho_X| \propto (p - p_1)^{\beta_X}, \quad (6)$$

where ρ_X^{sat} is the saturation concentration. Note that the saturation concentration for active sites and A is zero, whereas it is non-zero for B and empty sites. Thus we assume that the density of various sites depends on system size and distance from the critical point as:

$$|\rho_X^{sat}(p, L) - \rho_X(p, L)| \propto L^{-\beta/\nu_\perp} \mathcal{F}(\Delta L^{1/\nu_\perp}), \quad (7)$$

such that at the critical point p_1

$$|\rho_X^{sat}(p_1, L) - \rho_X(p_1, L)| \propto L^{-\beta/\nu_\perp}. \quad (8)$$

ρ_X , and other quantities, are averaged over the *surviving* samples only. Fig. 2 shows a plot of the average concentration of sites $\log_2 |\rho_X^{sat}(p_1, L) - \rho_X(p_1, L)|$ as a function of $\log_2 L$ at the critical point, $p_1 = 0.3422$. All simulations were performed on lattices of size $L \times L$ using periodic boundary conditions. The maximal number of timesteps in each trial, t_M , and number independent samples, N_S , varied from $t_M = 150$, $N_S = 50,000$ for $L = 8$ to $t_M = 75,000$, $N_S = 500$ for $L = 256$. The slope of the line drawn in the figure is $\beta/\nu_\perp = 0.81$, which comes from the DP estimate $\beta/\nu_\perp = 0.81(2)$, using the earlier cited estimate for β and $\nu_\perp = 0.729(8)$ [25]. The data falls very nicely on the line drawn using the DP estimate thus confirming that the model belongs to the DP universality class.

Near the critical point the order parameter fluctuations grow like a power law, $\chi = L^d(\langle \rho^2 \rangle - \langle \rho \rangle^2) \propto \Delta^\gamma$, from which we expect the following finite-size scaling form,

$$\chi(p, L) \propto L^{\gamma/\nu_\perp} \mathcal{G}(\Delta L^{1/\nu_\perp}), \quad (9)$$

such that at p_1

$$\chi(p_1, L) \propto L^{\gamma/\nu_\perp}. \quad (10)$$

Fig. 3 shows a plot of $\log_2[\chi(p_1, L)]$ vs $\log_2 L$, as obtained from the fluctuations of the number of active sites. The slope of the straight line is 0.39 as obtained from the DP value $\gamma/\nu_\perp = 0.39(2)$, where I used that $\gamma = \gamma^{DP} - \nu_\parallel = 0.285(11)$ with $\gamma^{DP} = 1.571(6)$ [25]. The excellent agreement between the data and the DP-expectation confirms the DP critical behavior of this model.

One expects a characteristic time for the system, say the relaxation time, to scale like

$$\tau(p, L) \propto L^{-\nu_\parallel/\nu_\perp} \mathcal{T}(\Delta L^{1/\nu_\perp}), \quad (11)$$

such that at p_1

$$\tau(p_1, L) \propto L^{-\nu_\parallel/\nu_\perp}. \quad (12)$$

In Fig. 4 I have plotted $\log_2[\tau_h(p_1, L)]$, where τ_h is the time it takes for half the samples to enter an absorbing state, as a function of $\log_2 L$. The slope of the line drawn in the figure is $\nu_\parallel/\nu_\perp = 1.764$, as obtained from the DP estimate [25] $\nu_\parallel/\nu_\perp = 1.764(7)$. The DP estimate is derived from the scaling relation $\nu_\parallel/\nu_\perp = 2/z$ using the earlier cited estimate for z . As can be seen the data for the dimer-trimer model is again fully compatible with DP critical behavior.

3.3 Steady state behavior.

Finally I have studied the steady state behavior of the density of sites. As mentioned earlier $|\rho_X^{sat} - \rho_X|$ should go to zero like a power-law at p_1 . In Fig. 5 I have plotted these quantities as a function of the distance from the critical point on a log-log scale, using $\rho^{sat} = 0.8935$ for B particles and 0.1065 for isolated empty sites. The results were obtained by averaging over typically 100 independent samples. The number of time steps and system sizes varied from $t = 1000$, $L = 64$ far from p_1 to $t = 500,000$, $L = 512$ closest to p_1 . The slope of the straight line is 0.59 as obtained from the DP estimate. From this figure it is clear that all densities have the same asymptotic power-law behavior and once again confirm that the model belongs to the DP universality class.

4 Summary and discussion

Previous studies of various two-component models in two dimensions exhibiting a continuous phase transition into a non-unique absorbing state [17, 18, 19], yielded non-DP behavior. However, with the results reported in the previous section and in an earlier article [23], it is now clear that of these both the dimer-trimer model [17] and the CO-NO model [19] belong to the DP universality class. Likewise, results for the one-dimensional versions of the pair contact process [20, 21], dimer reaction model [21] and the threshold transfer process [22] clearly placed these models in the DP universality class. In all of these models the absorbing states can be uniquely characterized by the vanishing of a single quantity. More and more evidence thus confirm that the DP conjecture can be extended to such models, as first suggested in Ref. [21]. The exponent estimates for the various versions of the dimer-dimer model are not consistent with directed percolation. However, the typical value for $\beta \simeq 1/2$ (with an uncertainty of $\simeq 10\%$) is not very far from the DP value. In view of this, and the similarity of these models to the dimer-trimer and CO-NO models, it does not seem unlikely that the DD models also belong to the DP universality class.

References

- [1] Several articles about directed percolation may be found in *Percolation Structures and Processes*, edited by G. Deutsher, R. Zallen, and J. Adler, Annals of the Israel Physical Society Vol. 5 (Hilger, Bristol, 1983).
- [2] V. N. Gribov, Sov. Phys. JETP **26**, 414 (1968); V. N. Gribov and A. A. Migdal, Sov. Phys. JETP **28**, 784 (1969).
- [3] R. C. Brower, M. A. Furman, and M. Moshe, Phys. Lett. B **76**, 213 (1978).
- [4] T. E. Harris, Ann. Prob. **2**, 969 (1974).
- [5] P. Grassberger and A. de la Torre, Ann. Phys. (NY) **122**, 373 (1979).
- [6] F. Schlögl, Z. Phys. B **253**, 147 (1972).
- [7] H. K. Janssen, Z. Phys. B **42**, 151 (1981).
- [8] P. Grassberger, Z. Phys. B **47**, 365 (1982).
- [9] R. M. Ziff, E. Gulari, and Y. Barshad, Phys. Rev. Lett. **56**, 2553 (1986).
I. Jensen, H. C. Fogedby and R. Dickman, Phys. Rev. A **41**, 3411 (1991).
- [10] R. Bidaux, N. Boccara, and H. Chaté, Phys. Rev. A **39**, 3094 (1989).
I. Jensen, Phys. Rev. A **43**, 3187 (1991).
- [11] T. Aukrust, D. A. Browne, and I. Webman, Phys. Rev. A **41**, 5294 (1990)
- [12] R. Dickman, Phys. Rev. A **42**, 6985 (1990).
- [13] R. Dickman and Tania Tomé, Phys. Rev. A **44**, 4833 (1991).
- [14] H. Takayasu and A. Yu Tretyakov, Phys. Rev. Lett. **68** 3060 (1992).
I. Jensen, Phys. Rev E **47**, R1 (1993).
I. Jensen, J. Phys. A **26**, 3921 (1993).
- [15] H. Park, J. Köhler, I-M Kim, D. ben-Avraham, and S. Redner, J. Phys. A **26**, 2071 (1993).
- [16] J. Zhuo, S. Redner, and H. Park, J. Phys. A **26**, 4197 (1993).
- [17] J. Köhler and D. ben-Avraham, J. Phys. A **24**, L621 (1991); D. ben-Avraham and J. Köhler, J. Stat. Phys. **65**, 839 (1991).
- [18] E. V. Albano, J. Phys. A **25**, 2557 (1992); A. Maltz and E. V. Albano, Surf. Science **277**, 414 (1992); E. V. Albano, J. Stat. Phys. **69**, 643 (1992).
- [19] K. Yaldram, K. M. Khan, N. Ahmed, and M. A. Kkan, J. Phys. A **26**, L801 (1993).

- [20] I. Jensen, Phys. Rev. Lett. **70**, 1465 (1993).
- [21] I. Jensen and R. Dickman, Phys. Rev. E **48**, 1710 (1993).
- [22] J. F. F. Mendes, R. Dickman, M. Henkel, and M. C. Marques, *Generalized Scaling for Models with Multiple Absorbing States*, preprint 1993 cond-mat/9312028, to appear in J. Phys. A.
- [23] I. Jensen, J. Phys. A **27**, L61 (1994).
- [24] G. Grinstein, Z. W. Lai, and D. Browne, Phys. Rev. A **40**, 4820 (1989).
- [25] P. Grassberger, J. Phys. A **22**, 3673 (1989).

Figure Captions

Figure 1 Local slopes $-\delta(t)$ (upper panel), $\eta(t)$ (middle panel), and $z(t)$ (lower panel), as defined in Eq. 5 with $m = 5$. Each panel contains four curves with, from bottom to top, $p = 0.3418, 0.3420, 0.3422$ and 0.3424 .

Figure 2 The concentration of sites $\log_2 |\rho_X^{sat}(p_1, L) - \rho_X(p_1, L)|$ as a function of $\log_2 L$. The slope of the straight line is $\beta/\nu_\perp = 0.81$. Some of the densities have been scaled.

Figure 3 The fluctuations in the concentration of active sites $\log_2 [\chi(p_1, L)]$ vs $\log_2 L$. The slope of the straight line is $\gamma/\nu_\perp = 0.39$.

Figure 4 The time before *half* the samples enter an absorbing state $\log_2 [\tau_h(p_1, L)]$ vs $\log_2 L$. The slope of the straight line is $\nu_\parallel/\nu_\perp = 1.764$.

Figure 5 Log-log plot of $|\rho_X^{sat}(p_1, L) - \rho_X|$ as a function of the distance, $|p - p_1|$, from the critical point $p_1 = 0.3422$. The slope of the straight line is $\beta = 0.59$. Some of the densities have been scaled.

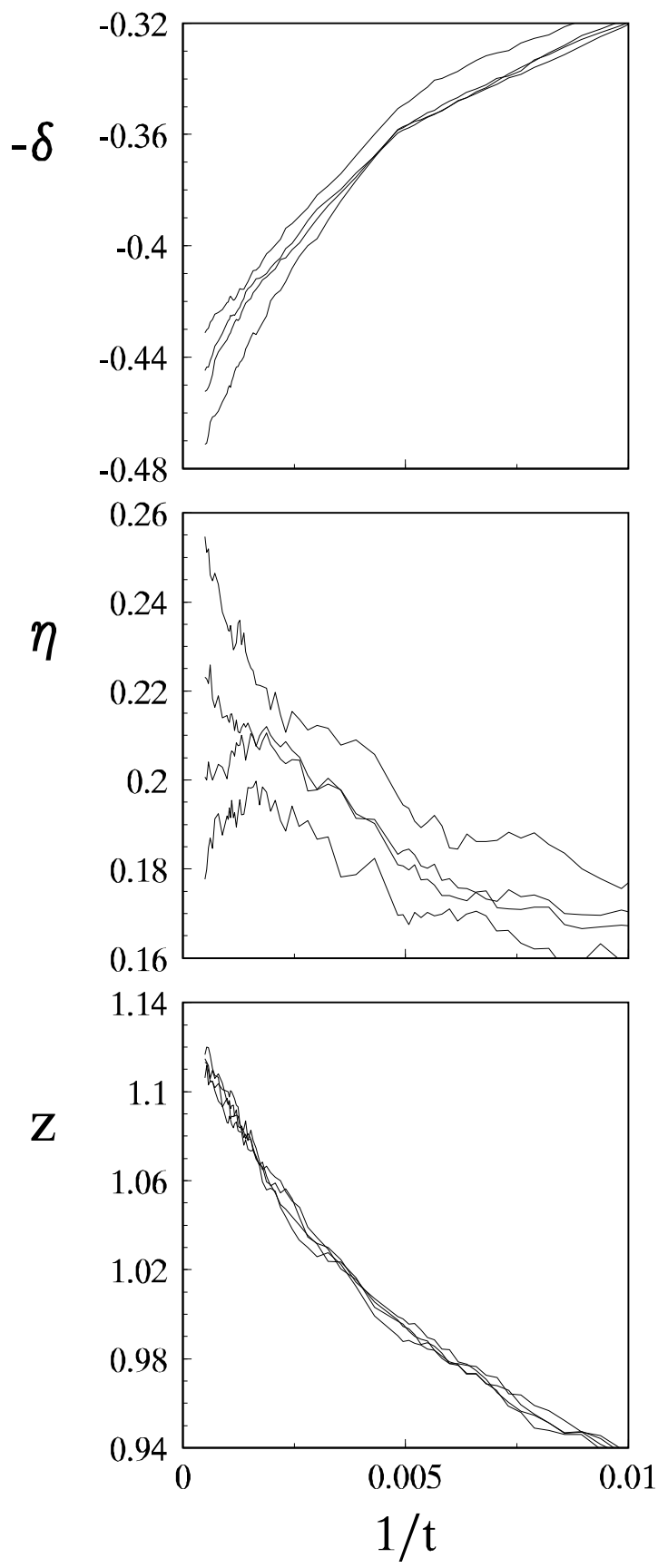


Fig. 1

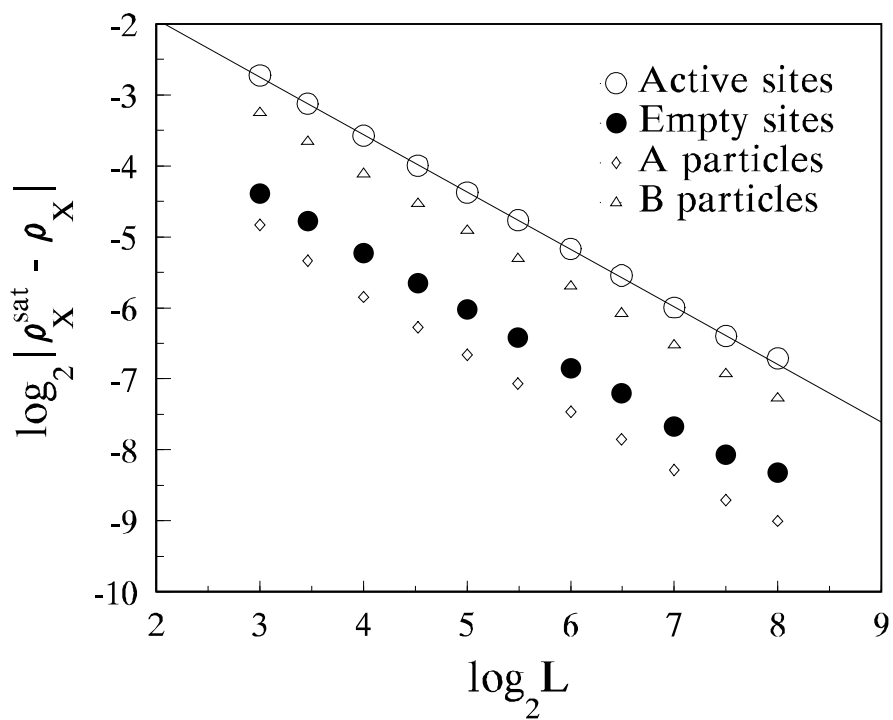


Fig. 2

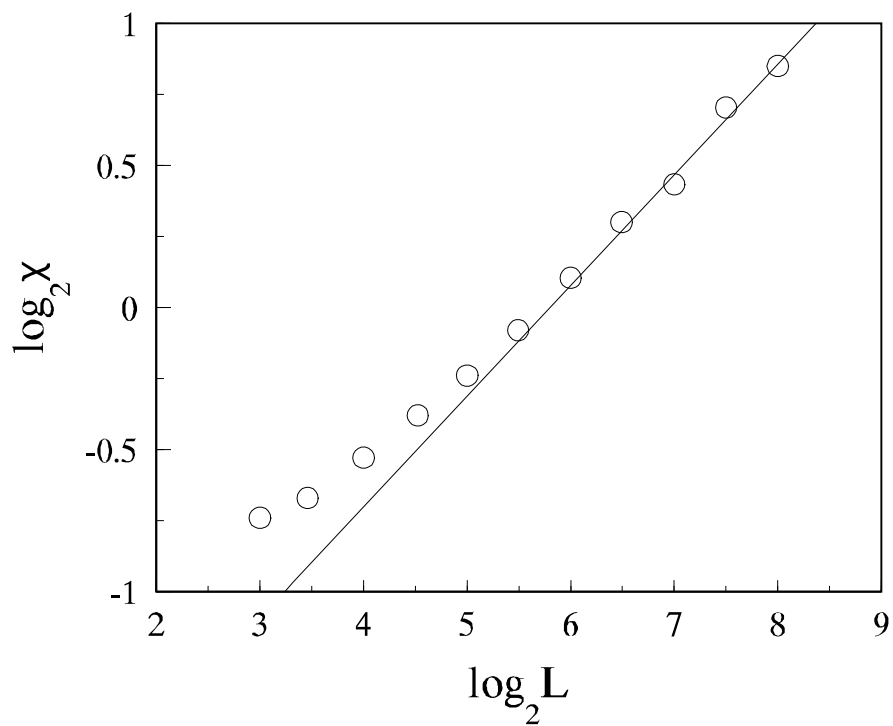


Fig. 3

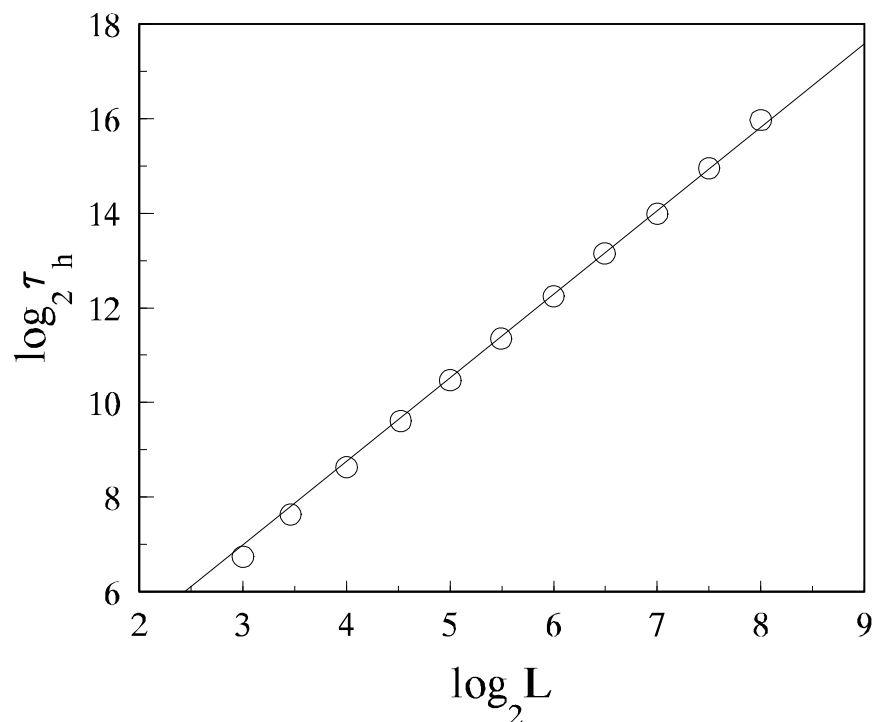


Fig. 4

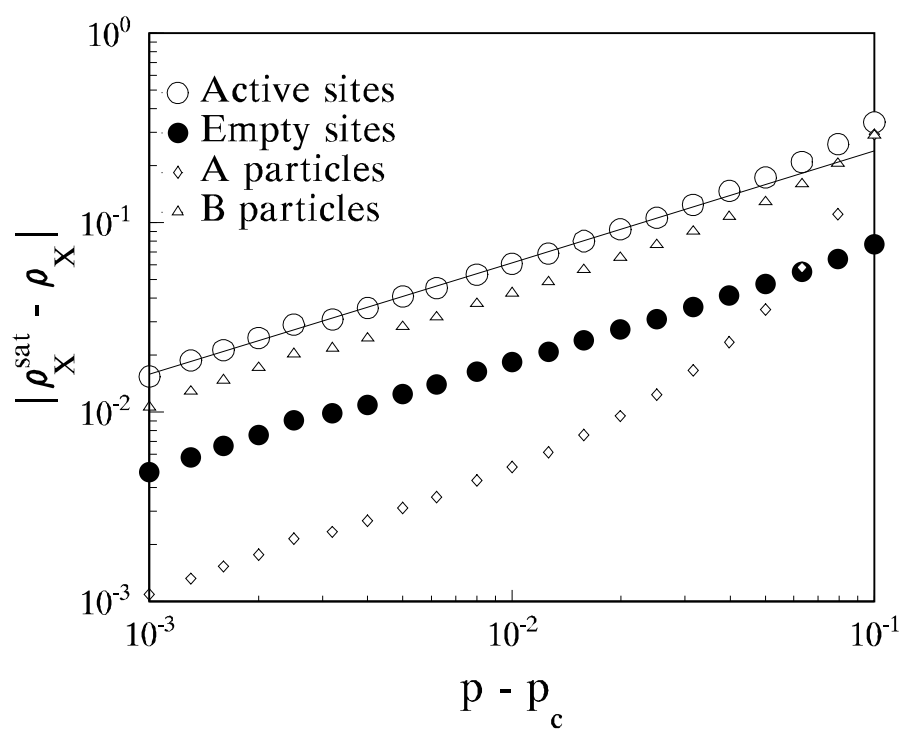


Fig. 5